Electronic supporting information for:

Photoinduced intersystem crossing in DNA oxidative lesions and epigenetic intermediates

Antonio Francés-Monerris,[a,b] *Mauricio Lineros-Rosa,*[c] *Miguel Angel Miranda,*[c] *Virginie Lhiaubet-Vallet,*[c,*] *Antonio Monari*[a,*]

[a]Université de Lorraine and CNRS, LPCT UMR 7019, F-54000 Nancy, France. [b]Departament de Química Física, Universitat de València, 46100 Burjassot, Spain. [c]Instituto Universitario Mixto de Tecnologia Química UPV-CSIC, Universitat Politècnica de València, Avda de los Naranjos s/n, 46022 Valencia, Spain.

Corresponding Authors

*V.L.-V. lvirgini@itq.upv.es, A.M. Antonio.monari@univ-lorraine.fr

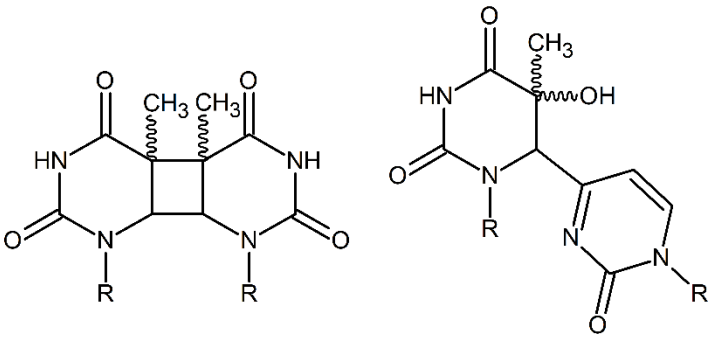

Figure S1) Structures of thymine-thymine CPD (left) and 64-PP (right).

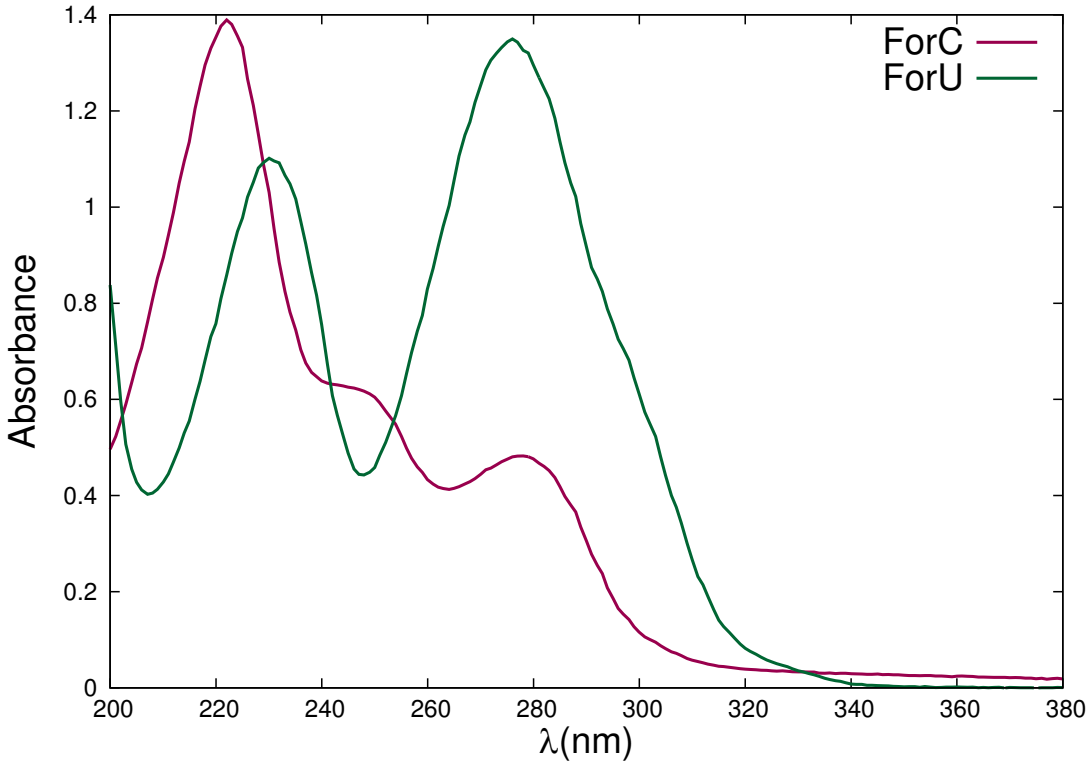

Figure S2) MilliQ absorption spectrum for ForU and ForC in water

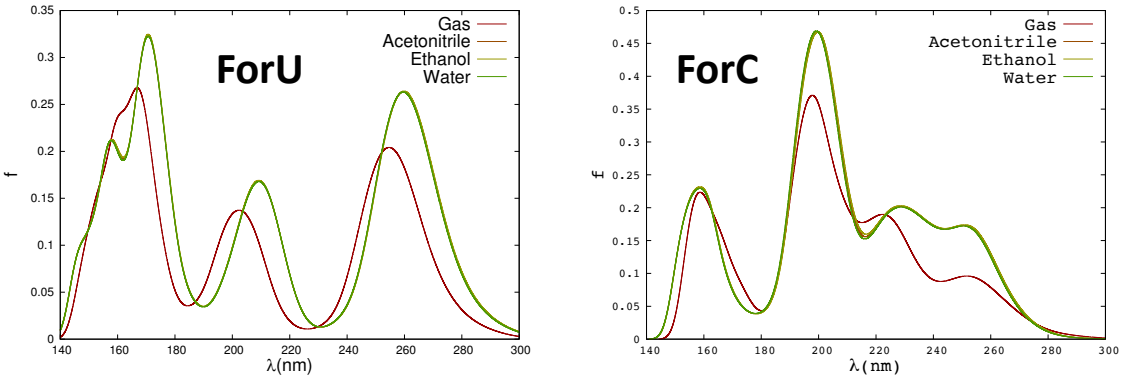

Figure S3) TD-DFT computed absorption spectra of ForU and ForC in different solvents

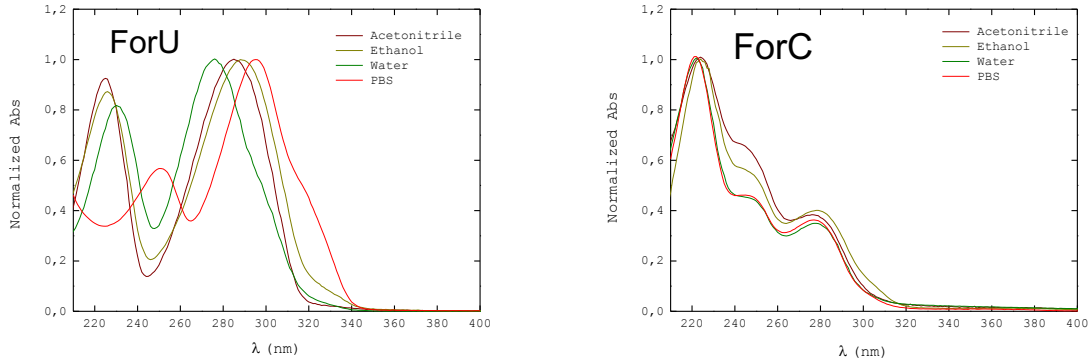

Figure S4) Experimental absorption spectra of ForU and ForC in different solvents

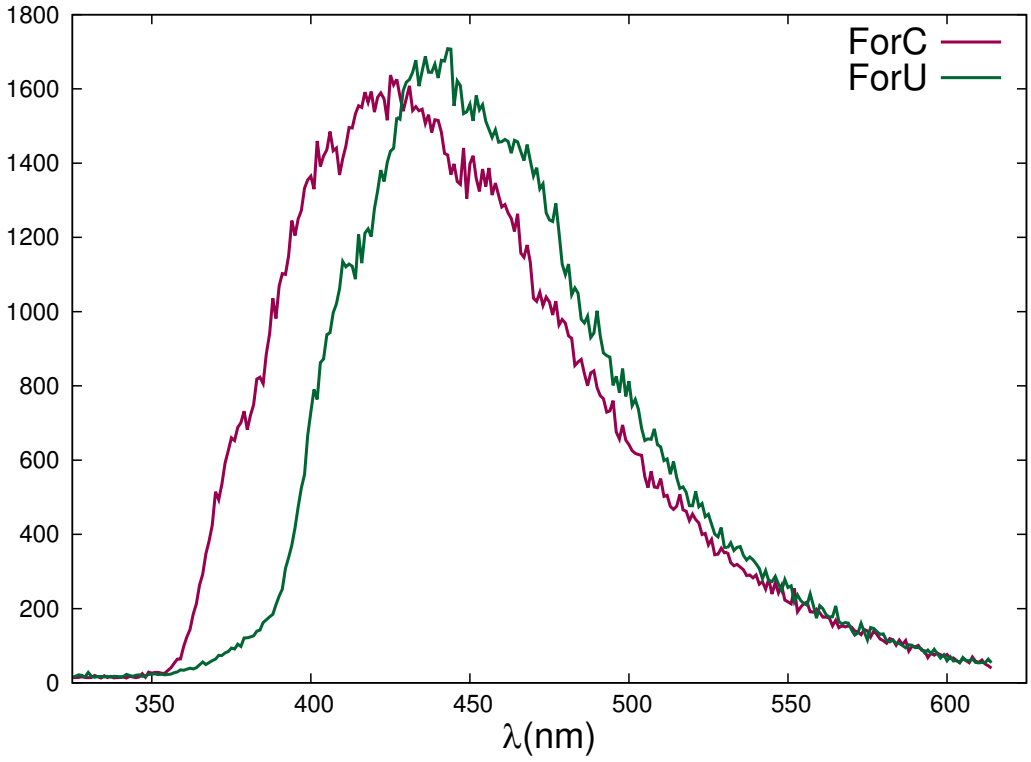

Figure S5) Low temperature phosphorescence spectra of ForC and ForU in Ethanol after excitation at 380 nm.

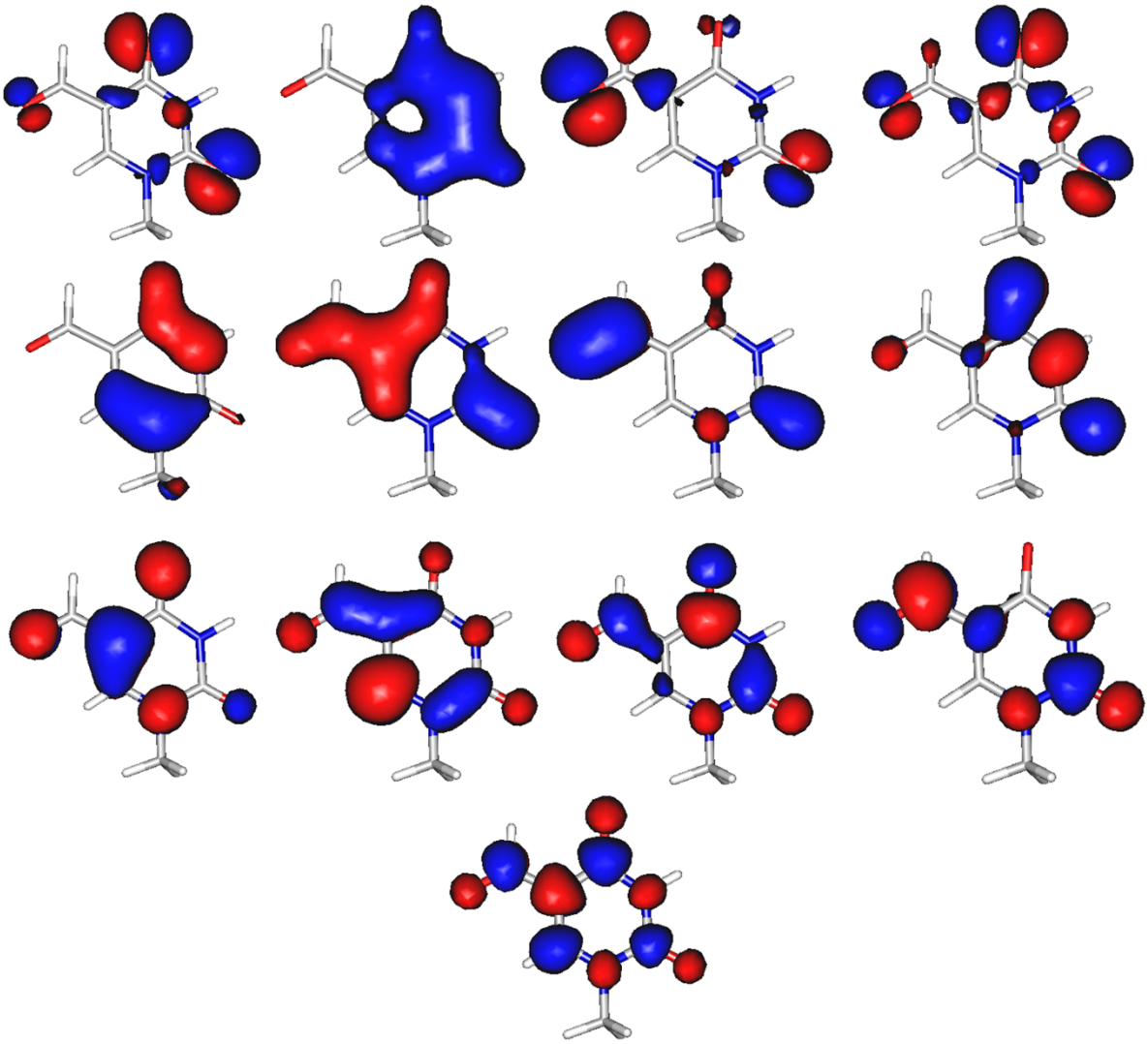

Figure S6) Active space orbitals for ForU

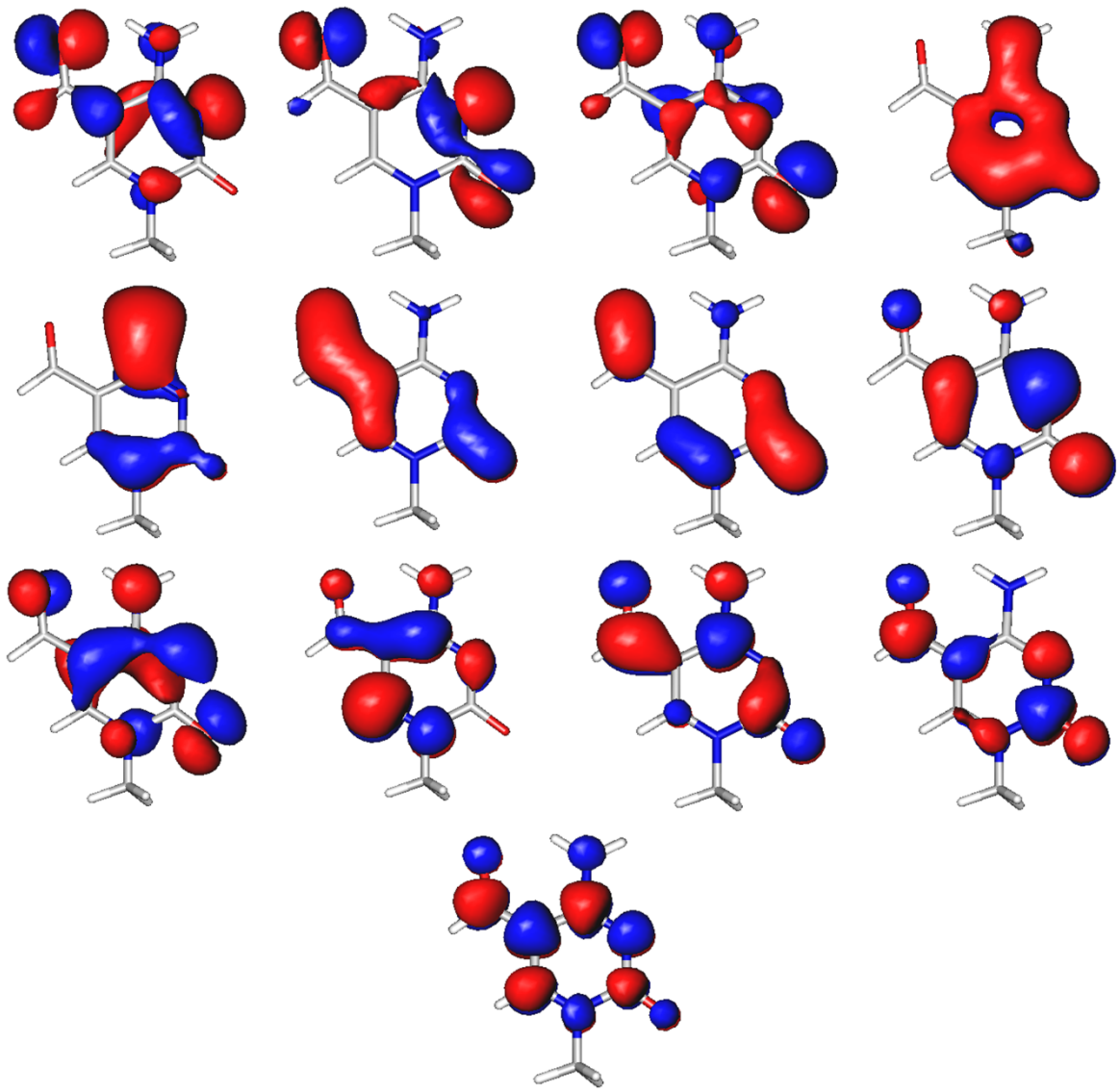

Figure S7) Active space orbitals for ForC

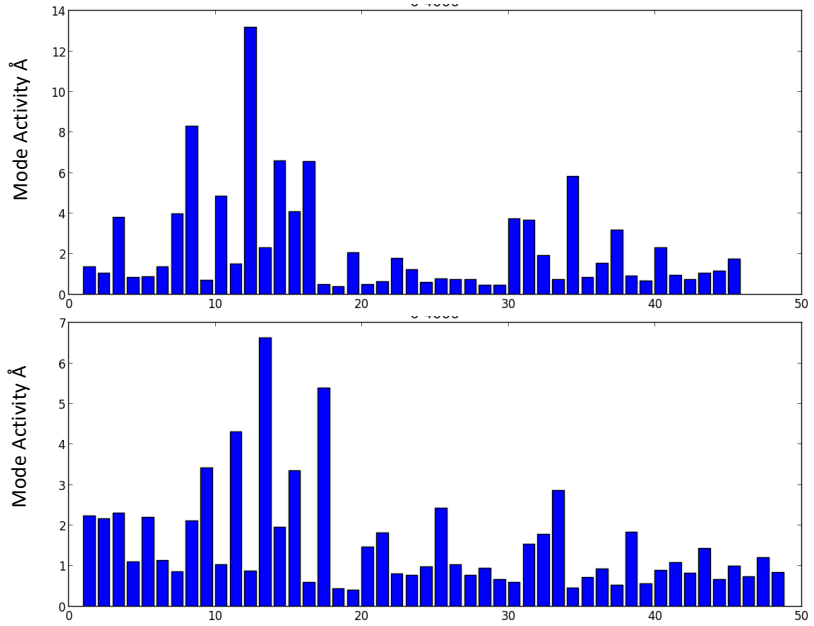

Figure S8) Total standard Deviation of the trajectories projected on the vibrational normal modes and yielding the total activity of each mode.

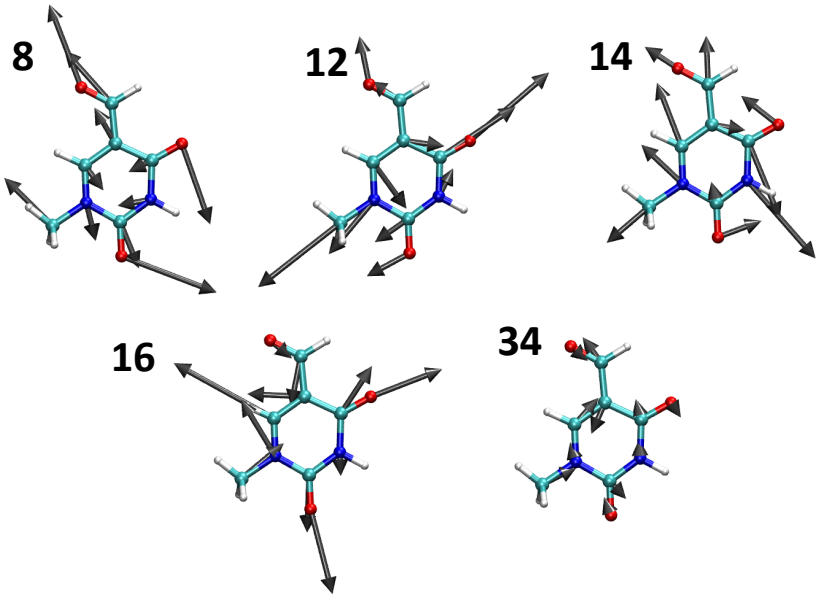

Figure S9) Representation of the ForU most active vibrational normal modes

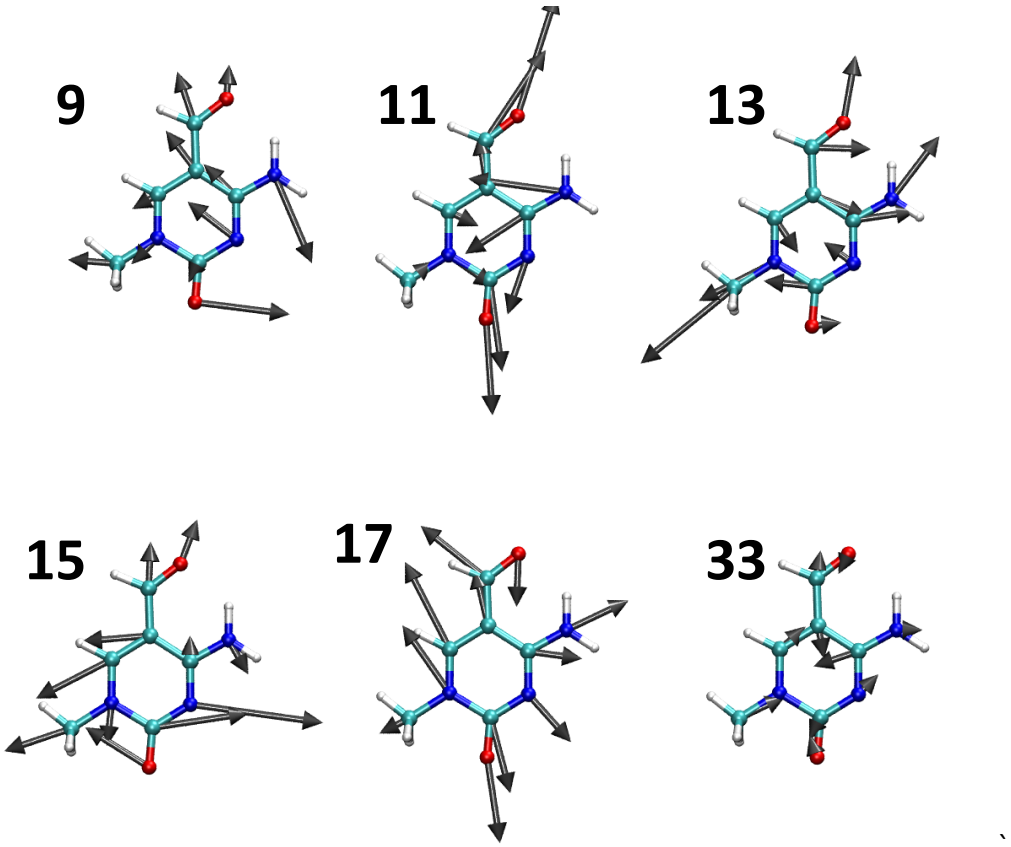

Figure S10) Representation of the ForC most active vibrational normal modes

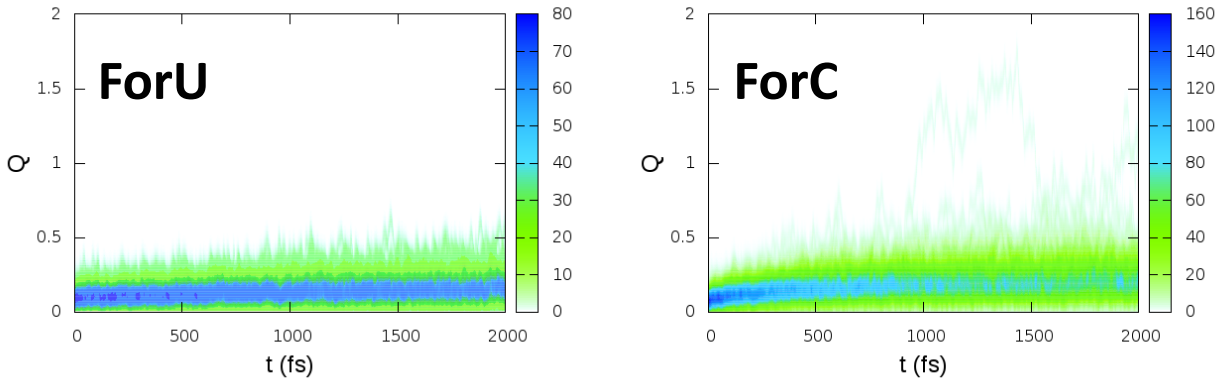

Figure S10) Time evolution of the aromatic ring puckering convoluted over the ensemble of the trajectories for ForU and ForC.

Methodology

Computational methodology

In all calculations, the models of ForU and ForC included a methyl group at N1 position as a substitute of the deoxyribose sugar of DNA. The Tamm-Dancoff approximation has been used in all TD-DFT calculations.

Absorption spectra. The ground state of the two chromophores has been optimized at the DFT level, using the B3LYP[1] functional and the Pople 6-31G+(d,p) basis set. The absorption spectra have been calculated with the TD-DFT method using a Wigner distribution around the S_0 minimum,[2] and convoluting the vertical excitations from 100 single points calculated at TD-DFT level with B3LYP and the 6-311G++(d,p) basis set, solvent effects have been taken into account using the linear response polarizable continuum model (PCM).[3] All the calculations have been performed with the Gaussian 09.D01 code.[4] The excited states have been characterized in terms of Natural Transition Orbitals (NTO) and ϕ_S index via the Nancy_EX code.[5]

PES exploration. According to a previous work,[6] the relevant points of the singlet and triplet PES have been optimized at the TD-DFT level making use of the ωB97-XD functional in combination with the 6-31+G(d,p) basis set and the Gaussian 09.D01 program. Since excited-state gradients for the ωB97-XD functional are not implemented in the Amsterdam Density Functional 2018 (ADF 2018) modelling suite,[7,8] and the studied photophysical processes do not involve intermolecular interactions such as π-stacking (that would require dispersion corrections) and/or long-range charge transfer states, we have computed the final energies shown in Figures 3B and 3D with the TD-B3LYP/DZ method as implemented in ADF 2018, which is available to perform non-adiabatic dynamics (see below).

All multiconfigurational calculations (Figures 3A and 3C) were conducted with the OpenMolcas software[9] on top of the ωB97-XD/6-31+G(d,p) optimized geometries. For both ForU and ForC systems, the complete-active-space self-consistent field (CASSCF) wave functions were built distributing 18 electrons into 13 orbitals (see ESI). Thus, the whole molecular valence space is included in the active space. Six roots were demanded in the state-average (SA)-CASSCF procedure for both singlet and triplet states calculations. The necessary electronic dynamic correlation was included by means of the complete-active-space second-order perturbation theory (CASPT2) method, using an imaginary level shift of 0.2 to avoid the presence of weakly intruder states, and an IPEA shift of 0.0 a.u., as previously used in the literature for related systems.[6,10,11]

Phosphorescent states. The vertical emission wavelengths and adiabatic energies reported in Table 1 were computed at the $^3n\pi^*$ and $^3\pi\pi^*$ minima of ForU and the $^3\pi\pi^*$ equilibrium geometry of ForC (Figure 3) including singlet-triplet SOCs. The SOC operator has been applied to scalar relativistic TD-B3LYP/TZP calculations by means of perturbation theory mixing ten singlet and ten triplet excited states. Solvent effects (ethanol) have been included by means of the COSMO method using the ADF 2018 default settings.

Non-adiabatic dynamics. Non-adiabatic dynamics have been performed in the state-hopping formalism using the Sharc 2.0 code[12,13] interfaced with the ADF 2018 modelling suite.[7,8] The latter has been used to calculate the electronic structure and the relevant couplings, TD-DFT has been consistently used with the B3LYP functional and the Slater-type DZ basis set. This level of theory has been chosen because it reproduces the *ab-initio* profiles while making the dynamics affordable. 100 trajectories departing from S_1 have been run for ForU, whereas 100 runs starting from S_1 and 100 trajectories starting from S_2 have been calculated for ForC due to the closer degeneracy of the first two singlet excited states and the similar values of their oscillator strengths. The runs have been propagated with a time step of 0.5 fs for a total time of 2.0 ps using the full-diagonal representation, a Tully based stochastic hopping protocol,[14] and the Granucci, Persico and Zoccante decoherence correction,[15] the wavefunction overlap approach has been used to compute the non-adiabatic couplings on the fly.[16]

Experimental methodology

Chemicals. The chemicals 5-formylcytosine (Toronto Research Chemicals, ≥97%) and 5-formyluracil (Sigma-Aldrich, ≥98%) were used as received. Ethanol and acetonitrile of HPLC grade were purchased from Scharlau, whereas water was purified using Milli-Q system (IQ 7000, Merck). Phosphate buffered saline (PBS) tablets were purchased from Sigma Aldrich and used as received to prepare PBS solutions in Milli-Q water at pH 7.4 at 25ºC.

UV–vis Absorption. Solutions of ForU and ForC were prepared in PBS, MeCN or EtOH, and UV absorption spectra were registered on a Cary 50 spectrophotometer (Varian) using a quartz cuvette of 1 cm optical path and 3 mL capacity.

Phosphorescence Emission. The phosphorescence experiments were performed using ethanol solutions of ForU and ForC and adjusting their absorbance at ca. 0.8 (value determined for a 1 cm optical path) at the excitation wavelength of 280 nm. Solutions were then transferred to quartz tubes of 5 mm diameter. The emission was measured at 77 K, a gate time of 50 μs, and a delay of 500 μs.

References

1 A. Becke, *J. Chem. Phys.*, 1993, **98**, 5648–5652.

2 J. P. Dahl and M. Springborg, *J. Chem. Phys.*, 1988, **88**, 4535–4547.

3 B. Mennucci, *Wiley Interdiscip. Rev. Comput. Mol. Sci.*, 2012, **2**, 386–404.

4 M. J. Frisch, G. W. Trucks, H. B. Schlegel, G. E. Scuseria, M. A. Robb, J. R. Cheeseman, G. Scalmani, V. Barone, B. Mennucci, G. A. Petersson, H. Nakatsuji, M. Caricato, X. Li, H. P. Hratchian, A. F. Izmaylov, J. Bloino, G. Zheng, J. L. Sonnenberg, M. Hada, M. Ehara, K. Toyota, R. Fukuda, J. Hasegawa, M. Ishida, T. Nakajima, Y. Honda, O. Kitao, H. Nakai, T. Vreven, J. A. Montgomery Jr., J. E. Peralta, F. Ogliaro, M. Bearpark, J. J. Heyd, E. Brothers, K. N. Kudin, V. N. Staroverov, R. Kobayashi, J. Normand, K. Raghavachari, A. Rendell, J. C. Burant, S. S. Iyengar, J. Tomasi, M. Cossi, N. Rega, J. M. Millam, M. Klene, J. E. Knox, J. B. Cross, V. Bakken, C. Adamo, J. Jaramillo, R. Gomperts, R. E. Stratmann, O. Yazyev, A. J. Austin, R. Cammi, C. Pomelli, J. W. Ochterski, R. L. Martin, K. Morokuma, V. G. Zakrzewski, G. A. Voth, P. Salvador, J. J. Dannenberg, S. Dapprich, A. D. Daniels, O. Farkas, J. B. Foresman, J. V Ortiz, J. Cioslowski and D. J. Fox, *Gaussian 09 Revis. D.01*, 2010, Gaussian Inc., Wallingford CT.

5 T. Etienne, X. Assfeld and A. Monari, *J. Chem. Theory Comput.*, 2014, **10**, 3896–3905.

6 A. Francés-Monerris, C. Hognon, M. A. Miranda, V. Lhiaubet-Vallet and A. Monari, *Phys. Chem. Chem. Phys.*, 2018, **20**, 25666–25675.

7 E. J. Baerends, T. Ziegler, A. J. Atkins, J. Autschbach, D. Bashford, O. Baseggio, A. Bérces, F. M. Bickelhaupt, C. Bo, P. M. Boerritger, L. Cavallo, C. Daul, D. P. Chong, D. V Chulhai, L. Deng, R. M. Dickson, J. M. Dieterich, D. E. Ellis, M. van Faassen, A. Ghysels, A. Giammona, S. J. A. van Gisbergen, A. Goez, A. W. Götz, S. Gusarov, F. E. Harris, P. van den Hoek, Z. Hu, C. R. Jacob, H. Jacobsen, L. Jensen, L. Joubert, J. W. Kaminski, G. van Kessel, C. König, F. Kootstra, A. Kovalenko, M. Krykunov, E. van Lenthe, D. A. McCormack, A. Michalak, M. Mitoraj, S. M. Morton, J. Neugebauer, V. P. Nicu, L. Noodleman, V. P. Osinga, S. Patchkovskii, M. Pavanello, C. A. Peeples, P. H. T. Philipsen, D. Post, C. C. Pye, H. Ramanantoanina, P. Ramos, W. Ravenek, J. I. Rodríguez, P. Ros, R. Rüger, P. R. T. Schipper, D. Schlüns, H. van Schoot, G. Schreckenbach, J. S. Seldenthuis, M. Seth, J. G. Snijders, M. Solà, S. M., M. Swart, D. Swerhone, G. te Velde, V. Tognetti, P. Vernooijs, L. Versluis, L. Visscher, O. Visser, F. Wang, T. A. Wesolowski, E. M. van Wezenbeek, G. Wiesenekker, S. K. Wolff, T. K. Woo and A. L. Yakovlev, .

8 G. te Velde, F. M. Bickelhaupt, E. J. Baerends, C. Fonseca Guerra, S. J. A. van Gisbergen, J. G. Snijders and T. Ziegler, *J. Comput. Chem.*, 2001, **22**, 931–967.

9 I. Fdez. Galván, M. Vacher, A. Alavi, C. Angeli, F. Aquilante, J. Autschbach, J. J. Bao, S. I. Bokarev, N. A. Bogdanov, R. K. Carlson, L. F. Chibotaru, J. Creutzberg, N. Dattani, M. G. Delcey, S. S. Dong, A. Dreuw, L. Freitag, L. M. Frutos, L. Gagliardi, F. Gendron, A. Giussani, L. González, G. Grell, M. Guo, C. E. Hoyer, M. Johansson, S. Keller, S. Knecht, G. Kovačević, E. Källman, G. Li Manni, M. Lundberg, Y. Ma, S. Mai, J. P. Malhado, P. Å. Malmqvist, P. Marquetand, S. A. Mewes, J. Norell, M. Olivucci, M. Oppel, Q. M. Phung, K. Pierloot, F. Plasser, M. Reiher, A. M. Sand, I. Schapiro, P. Sharma, C. J. Stein, L. K. Sørensen, D. G. Truhlar, M. Ugandi, L. Ungur, A. Valentini, S. Vancoillie, V. Veryazov, O. Weser, T. A. Wesołowski, P.-O. O. Widmark, S. Wouters, A. Zech, J. P. Zobel and R. Lindh, *J. Chem. Theory Comput.*, 2019, **15**, doi: 10.1021/acs.jctc.9b00532.

10 A. Frances-Monerris, J. Segarra-Marti, M. Merchan and D. Roca-Sanjuan, *Theor. Chem. Acc.*, 2016, **135**, 31.

11 A. Francés-Monerris, M. Merchán and D. Roca-Sanjuán, *J. Org. Chem.*, 2017, **82**, 276–288.

12 S. Mai, P. Marquetand and L. González, *Wiley Interdiscip. Rev. Comput. Mol. Sci.*, 2018, **8**, e1370.

13 S. Mai, P. Marquetand and L. González, *Int. J. Quantum Chem.*, 2015, **115**, 1215–1231.

14 J. C. Tully, *J. Chem. Phys.*, 1990, **93**, 1061–1071.

15 G. Granucci, M. Persico and A. Zoccante, *J. Chem. Phys.*, 2010, **133**, 134111.

16 F. Plasser, M. Ruckenbauer, S. Mai, M. Oppel, P. Marquetand and L. González, *J. Chem. Theory Comput.*, 2016, **12**, 1207–1219.